ELSEVIER

Journal of Power Sources 102 (2001) 130–134

JOURNAL OF POWER SOURCES

www.elsevier.com/locate/jpowsour

Effects of iron substitution for nickel on electrochemical properties of $LiNi_{0.8}Co_{0.2}O_2$ for lithium rechargeable batteries

Sung-Chul Park[a], Young-Soo Han[a], Paul S. Lee[a], Soonho Ahn[b], Hyang-Mok Lee[b], Jai-Young Lee[a,*]

[a]*Department of Materials Science and Engineering, Korea Advanced Institute of Science and Technology, 373-1 Kusong-Dong, Yusong-Gu, Taejon 305-701, South Korea*

[b]*LG Chemical Ltd., Research Park, Science Town, Taejon 305-380, South Korea*

Received 10 November 2000; received in revised form 20 December 2000; accepted 4 May 2001

Abstract

Iron was substituted for Ni in $LiNi_{0.8}Co_{0.2}O_2$ in order to enhance its electrochemical properties such as cycle life and rate capability. $LiNi_{0.8-x}Fe_xCo_{0.2}O_2$ ($0 \leq x \leq 0.1$) was synthesized in flowing oxygen for 12–48 h at 650–800°C, and its structural and electrochemical properties were characterized with X-ray diffraction (XRD), cyclic voltammetry (CV) and charge–discharge tests. The XRD patterns of $LiNi_{0.8-x}Fe_xCo_{0.2}O_2$ showed that the α-$NaFeO_2$ type layered structure was maintained up to $x = 0.1$. As Fe was substituted for Ni up to $x = 0.05$, the rate capability of $LiNi_{0.8-x}Fe_xCo_{0.2}O_2$ was improved. $LiNi_{0.75}Fe_{0.05}Co_{0.2}O_2$ showed better cycle stability than $LiNi_{0.8}Co_{0.2}O_2$. XRD measurements indicated that the lattice of $LiNi_{0.75}Fe_{0.05}Co_{0.2}O_2$ expanded less than that of $LiNi_{0.8}Co_{0.2}O_2$ when the lithium was de-intercalated. CV curves of $LiNi_{0.8-x}Fe_xCo_{0.2}O_2$ showed current peaks, which are related to the phase transitions, diminished with Fe substitution during charging and discharging owing to the decrease of Ni^{3+}. Consequently, the improved cycle stability of $LiNi_{0.75}Fe_{0.05}Co_{0.2}O_2$ may be attributed to the decrease of phase transition.

Keywords: Lithium secondary battery; $LiNi_{1-x}Co_xO_2$; Iron substitution; Rate capability; Cycle life

1. Introduction

Rechargeable Li-ion batteries have important applications in portable electronic appliances such as cellular telephones, camcorders, and laptop computers. At present, most commercial Li-ion batteries use $LiCoO_2$ as cathode material because of its excellent cycle life although Co is a relatively rare and expensive transition metal [1,2]. Recently much attention has been paid to $LiNiO_2$ due to its advantages of low cost and potentially greater capacity compared to $LiCoO_2$ [3]. However, $LiNiO_2$ has the critical disadvantage of structural instability. Therefore, many researchers have intensively investigated $LiNi_{1-z}M_zO_2$ (M = Co, Al, Mn, Ti, and Fe) to improve the structural instability of $LiNiO_2$ by substituting any other transition metal for Ni [4–10]. In particular, $LiNi_{1-z}Co_zO_2$ ($0 < z < 1$) in solid solution is considered to be a most promising cathode material because the structural instability of $LiNiO_2$ is reduced by substituting Co for Ni. However, its cycle life and rate capability must be improved to complete with $LiCoO_2$. Nishida et al. [11] reported that Mn substitution for Ni in $LiNi_{1-z}Co_zO_2$ enhanced the electrochemical properties such as cycle life.

In the current work, $LiNi_{0.8-x}Fe_xCo_{0.2}O_2$ ($x \leq 0.1$) was synthesized and the effects of Fe on its electrochemical properties and structure were investigated.

2. Experimental

$LiNi_{0.8-x}Fe_xCo_{0.2}O_2$ ($0 \leq x \leq 0.1$) was prepared from $LiOH{\cdot}H_2O$, $Ni(NO_3)_2{\cdot}6H_2O$, $Co(NO_3)_2{\cdot}H_2O$, and $Fe(NO_3)_3{\cdot}9H_2O$. The reagents were thoroughly mixed in distilled water, dried in a vacuum oven, and then the mixture was pressed into pellets. The pellets were calcined for 6–24 h at 650–800°C in oxygen atmosphere. The calcined materials were ground, pressed into pellets and then reacted for 6–24 h at 650–800°C in oxygen. The reaction product was ground and screened between 325 and 500 mesh sieves.

For structural analysis, samples were characterized with X-ray diffraction (XRD) with Cu Kα radiation (Rigaku D/MAX-IIIC). The as-prepared samples were classified into two types of powder with sieves (325 and 500 mesh). The first is powder screened between sieves of 325 and

* Corresponding author. Tel.: +82-42-869-3313; fax: +82-42-869-8910.
E-mail address: jailee@mail.kaist.ac.kr (J.-Y. Lee).

0378-7753/01/$ – see front matter
PII: S0378-7753(01)00780-7

500 mesh, and the other is powder passing through a 500 mesh sieve. The particle size was measured with particle measuring and analysis system (PAMAS) and a scanning electronic microscope (SEM).

Positive electrodes were prepared by coating the mixture of the active material (88 wt.%), acetylene black (7 wt.%) as a conductive agent, and polyvinylidene fluoride (PVDF; 5 wt.%) as a binder dissolved in *N*-methyl pyrrolidinone on Al foil. After coating, the electrodes were dried at 140°C for 2 h in vacuum (10^{-3} Torr) and then pressed at about 150 kg/cm^2.

The components were fabricated into coin-type cells in an argon-filled glove box, where the counter electrode was Li metal and the electrolyte was 1 M $LiPF_6$ dissolved in a 50/50 vol.% mixture of ethylene carbonate (EC) and diethyl carbonate (DEC). A microporous film (Celgard 2400) was used as a separator. These cells were charged and discharged at a constant current density in the range of 18–360 mA/g (0.1–2 C rate) using Toyo Cycler. Potentiostatic charge–discharge tests were carried out with cyclic voltammetry (CV) at a scan rate of 0.01 V/s.

3. Results and discussion

3.1. Structural characterization of $LiNi_{0.8-x}Fe_xCo_{0.2}O_2$ ($0 \leq x \leq 0.1$)

The capacity of $LiNi_{0.8}Co_{0.2}O_2$ synthesized at 650–800°C for 12–48 h was measured to decide the synthesis condition. Fig. 1 shows the capacity change of $LiNi_{0.8}Co_{0.2}O_2$ with variation of synthesis temperature and time. The maximum discharge capacity and the minimum irreversible capacity was obtained from samples synthesized at 750°C for 24 h in oxygen atmosphere. The capacity decreases when the sample is prepared above 800°C or at 750°C for more than 36 h. XRD patterns for $LiNi_{0.8-x}Fe_xCo_{0.2}O_2$ ($x = 0$, 0.05, 0.07, and 0.1) obtained after firing at 750°C for 24 h in oxygen atmosphere are shown in Fig. 2. Although Fe is replaced up to x[Fe] = 0.1 mole fraction, all samples maintain the hexagonal structure (α-$NaFeO_2$).

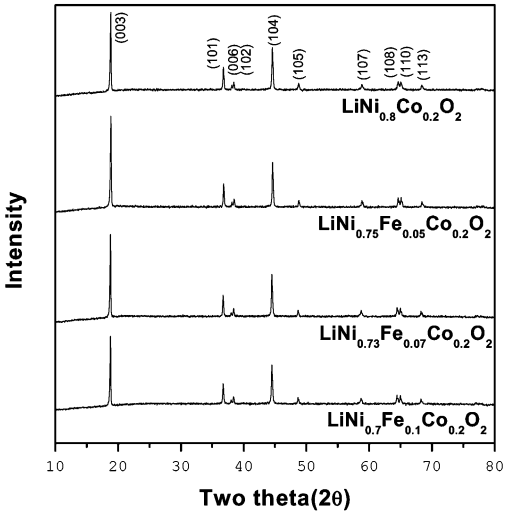

Fig. 2. XRD patterns of $LiNi_{0.8-x}Fe_xCo_{0.2}O_2$ ($x = 0$, 0.05, 0.07, and 0.1) prepared for 24 h at 750°C.

It is believed that the electrochemical properties of a cathode material are affected by the particle size [12,13]. As the particle size decreases, the capacity and cycle life are reported to increase. In this study, powders which are screened with sieves between 325 and 500 mesh are mainly used to exclude the particle size effect among as-prepared materials. Table 1 shows the effective particle size of the screened powders. This result indicates that the screened powders have the similar distribution of particle size.

3.2. Electrochemical characterization of $LiNi_{0.8-x}Fe_xCo_{0.2}O_2$ ($0 \leq x \leq 0.1$)

Fig. 3 shows the variation of discharge capacity for several $LiNi_{0.8-x}Fe_xCo_{0.2}O_2$ ($x = 0$, 0.02, 0.05, 0.07, and

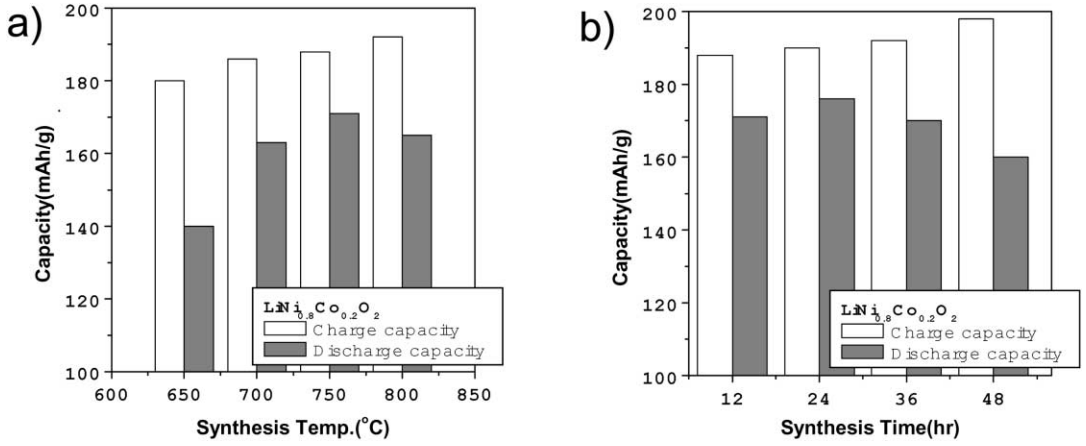

Fig. 1. Capacity change of $LiNi_{0.8}Co_{0.2}O_2$ vs. (a) synthesis temperature, (b) time: (a) samples were synthesized for 12 h at 650–800°C and (b) samples were synthesized for 12–48 h at 750°C. The capacity was measured at a rate of 18 mA/g (0.1 C rate) between 2.5 and 4.3 V.

Table 1
The effective particle size of powders screened between sieves of 325 and 500 mesh

Composition	Effective particle size (μm)
$LiNi_{0.8}Co_{0.2}O_2$	33.25
$LiNi_{0.75}Fe_{0.05}Co_{0.2}O_2$	34.84
$LiNi_{0.7}Fe_{0.1}Co_{0.2}O_2$	35.68

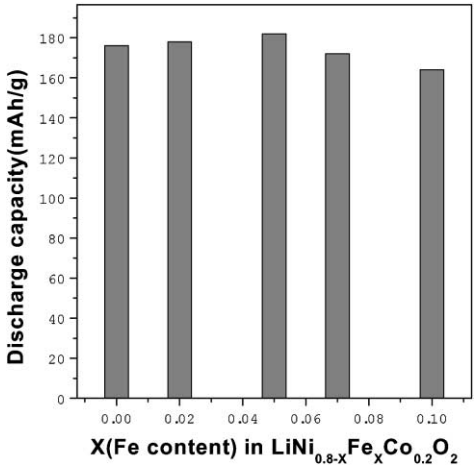

Fig. 3. Discharge capacity of $LiNi_{0.8-x}Fe_xCo_{0.2}O_2$ with respect to iron content at the rate of 18 mA/g (0.1 C rate) between 2.5 and 4.3 V.

0.1). It is found that the capacity of $LiNi_{0.8-x}Fe_xCo_{0.2}O_2$ is maintained when Fe is substituted up to $x[Fe] = 0.05$. With increasing amount of Fe above $x[Fe] = 0.05$, the discharge capacity decreases. The variation of rate capability in $LiNi_{0.8-x}Fe_xCo_{0.2}O_2$ is shown in Fig. 4. The rate capability is defined as the capacity at a rate of 180 mA/g (1 C rate) divided by the capacity at a rate of 36 mA/g (0.2 C rate). The gray column indicates the rate capability of samples screened between 325 and 500 mesh sieves. The white column shows the rate capacity of samples passing through 500 mesh sieve. As shown in Fig. 4, smaller samples have

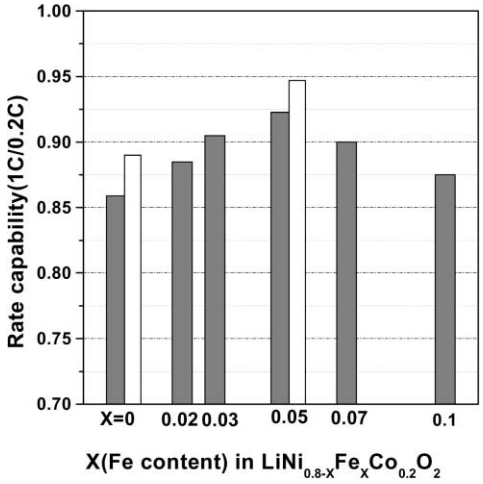

Fig. 4. Change of rate capability of $LiNi_{0.8-x}Fe_xCo_{0.2}O_2$ with respect to iron content: gray and white columns represent the rate capability of samples screened between sieves of 325 and 500 mesh and samples passing through 500 mesh sieve, respectively.

higher rate capability due to the larger surface area and the shorter diffusion length. And the rate capability as a function of Fe content is maximized when $x[Fe] = 0.05$.

Fig. 5 shows the cycle life performance of $LiNi_{0.8-x}Fe_xCo_{0.2}O_2$ ($x = 0$ and 0.05) at a rate of 180 mA/g (1 C rate). The cells were cycled between 2.5 and 4.3 V. The capacity of $LiNi_{0.75}Fe_{0.05}Co_{0.2}O_2$ during cycling is significantly higher than that of $LiNi_{0.8}Co_{0.2}O_2$ as shown in Fig. 5a. This difference in capacity of $LiNi_{0.75}Fe_{0.05}Co_{0.2}O_2$ and $LiNi_{0.8}Co_{0.2}O_2$ results from the difference in rate capability. As the rate capability of $LiNi_{0.75}Fe_{0.05}Co_{0.2}O_2$ is higher than that of $LiNi_{0.8}Co_{0.2}O_2$, $LiNi_{0.75}Fe_{0.05}Co_{0.2}O_2$ shows a higher capacity at a high rate. Fig. 5b shows the normalized cycle life property (C/C_{max}), which confirms the fact that $LiNi_{0.75}Fe_{0.05}Co_{0.2}O_2$ has a better cycle stability than $LiNi_{0.8}Co_{0.2}O_2$. It is known that the cycle life is related to the stress-induced strain damage of cathode material. Recently, Wang et al. [14] suggested that the layered structure should

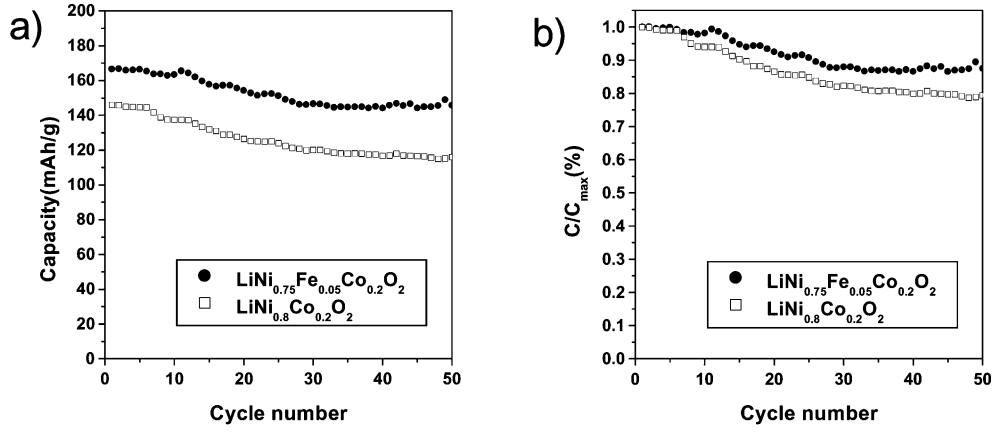

Fig. 5. (a) Cyclic performance, (b) normalized cyclic performance (C/C_{max}) of $LiNi_{0.75}Fe_{0.05}Co_{0.2}O_2$ and $LiNi_{0.8}Co_{0.2}O_2$ tested at a rate of 180 mA/g (1 C rate) between 2.5 and 4.3 V.

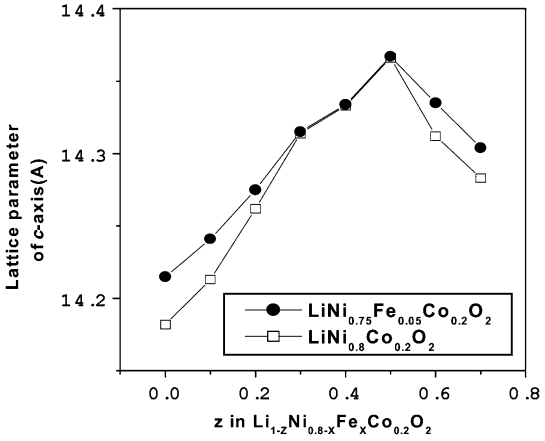

Fig. 6. Lattice expansions of $LiNi_{0.75}Fe_{0.05}Co_{0.2}O_2$ and $LiNi_{0.8}Co_{0.2}O_2$ during charging.

be degraded by the stress caused by lattice expansion during Li de-intercalation and Cho et al. [15] reported that the lattice change along the *c* direction caused fracture in the $LiNiO_2$ particles because this change exceeded the elastic strain tolerance of the oxides including the cathode materials. So, the lattice expansion of $LiNi_{0.8-x}Fe_xCo_{0.2}O_2$ ($x = 0$ and 0.05) during charging was measured and is shown in Fig. 6. When the lattice expansion of $LiNi_{0.75}Fe_{0.05}Co_{0.2}O_2$ and $LiNi_{0.8}Co_{0.2}O_2$ is compared, the former expands less than the latter. From this result, it can be speculated that the improved cycle life of $LiNi_{0.75}Fe_{0.05}Co_{0.2}O_2$ is attributed to the structural degradation reduced by the suppression of its lattice expansion. Dokko et al. [16] reported that the lattice change during the phase transition mostly influenced the capacity fading of the material. Therefore, the expansion and contraction of lattice may be related to the phase transition. In order to investigate the reason for the reduced lattice expansion in $LiNi_{0.75}Fe_{0.05}Co_{0.2}O_2$ during charging, the phase transition behaviors of $LiNi_{0.8-x}Fe_xCo_{0.2}O_2$ ($x = 0$, 0.05 and 0.1) was analyzed by CV curves. When the one phase is transformed to the other phase and the two phases coexists, the peak occurs in CV curves. That is, peaks in CV curves can be interpreted in terms of structural phase transitions [15,17]. Fig. 7 indicates that the intensity of the CV current peaks diminishes with increasing Fe content, which means that the phase transitions may be suppressed with the addition of Fe. The reason for the suppression of phase transitions with increasing Fe content can be understood by Ohzuku et al.'s study [3]. They reported that phase transitions shown in $LiNiO_2$ during cycling was probably due to the appearance and disappearance of the cooperative Jahn–Teller distortion of the NiO_6-octahedron. Therefore, the reason for the reduced phase transitions is that the amount of Ni^{3+} (which is Jahn–Teller ion) decreases with increasing Fe. It seems that the decrease of phase transition in $LiNi_{0.75}Fe_{0.05}Co_{0.2}O_2$ suppresses its lattice expansion in compared with $LiNi_{0.8}Co_{0.2}O_2$ and that the reduction of lattice expansion in $LiNi_{0.75}Fe_{0.05}Co_{0.2}O_2$ restrains the stress induced by lattice expansion and prevents the layered

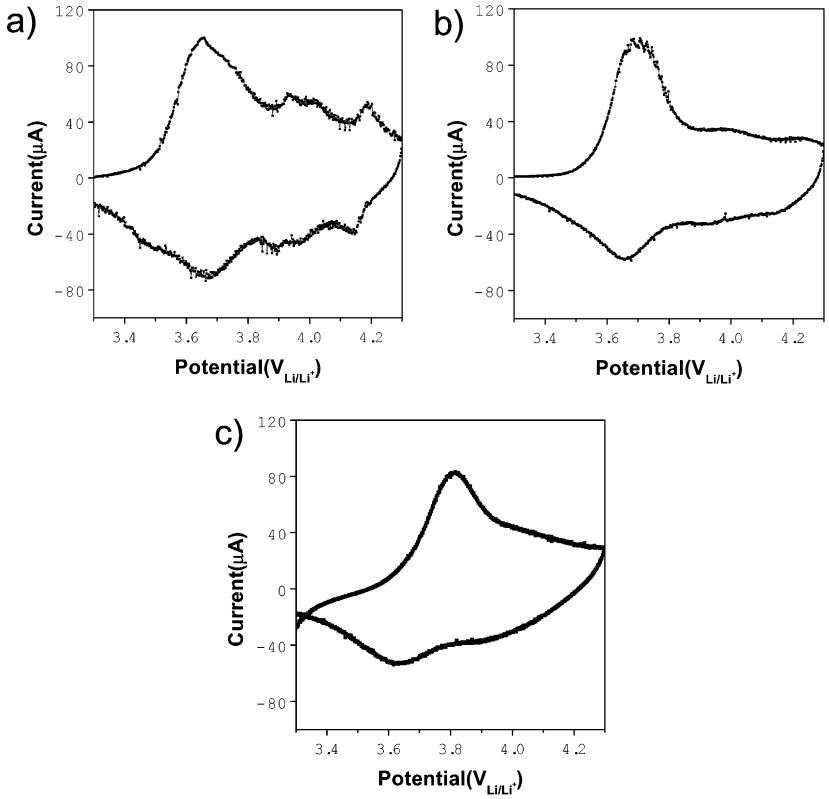

Fig. 7. Cyclic voltammetric curves of $LiNi_{0.8-x}Fe_xCo_{0.2}O_2$ during charging and discharging (scan rate: 0.01 V/s): (a) $x = 0$, (b) $x = 0.02$, and (c) $x = 0.05$.

structure from degrading. Consequently, the improved cycle stability of $LiNi_{0.75}Fe_{0.05}Co_{0.2}O_2$ may be attributed to the reduced phase transition.

4. Conclusions

$LiNi_{0.8-x}Fe_xCo_{0.2}O_2$ ($0 \leq x \leq 0.1$) was prepared in oxygen atmosphere for 12–48 h at 650–800°C. The maximum discharge capacity and the minimum irreversible capacity can be obtained from samples synthesized at 750°C for 24 h in flowing oxygen. $LiNi_{0.8-x}Fe_xCo_{0.2}O_2$ maintains a single phase of layered structure although 10 mol% of Fe is substituted. As Fe is substituted for Ni up to $x[\mathrm{Fe}] = 0.05$, the rate capability improves. $LiNi_{0.75}Fe_{0.05}Co_{0.2}O_2$ has better cycle stability than $LiNi_{0.8}Co_{0.2}O_2$ because the stress induced by lattice expansion may be relieved by the decrease of lattice expansion. The reason for the reduced lattice expansion is that the phase transition of $LiNi_{0.75}Fe_{0.05}Co_{0.2}O_2$ may be suppressed owing to the decrease of Ni^{3+} ion.

Acknowledgements

The authors wish to express thanks to the LG Chemical Ltd., Research Park for its partial financial support of this work.

References

[1] K. Ozawa, Solid State Ion. 69 (1994) 212.
[2] T. Ohzuku, A. Ueda, J. Electrochem. Soc. 141 (1994) 2972.
[3] T. Ohzuku, A. Ueda, M. Nagayama, J. Electrochem. Soc. 140 (1993) 1862.
[4] C. Delmas, I. Saadoune, A. Rougier, J. Power Sources 43/44 (1993) 595.
[5] A. Rougier, I. Saadoune, P. Gravereau, P. Willmann, C. Delmas, Solid State Ion. 90 (1996) 83.
[6] T. Ohzuku, A. Ueda, M. Kouguchi, J. Electrochem. Soc. 142 (1995) 4033.
[7] M. Yoshio, Y. Todorov, K. Yamato, H. Noguchi, J.-I. Itoh, M. Okada, T. Mouri, J. Power Sources 74 (1998) 46.
[8] M. Okada, K.-I. Takahashi, T. Mouri, J. Power Sources 68 (1997) 545.
[9] H. Arai, S. Okada, Y. Sakurai, J.I. Yamaki, J. Electrochem. Soc. 144 (1997) 3117.
[10] J.N. Reimers, E. Rossen, C.D. Jones, J.R. Dahn, Solid State Ion. 61 (1993) 335.
[11] N. Nishida, H. Fujimoto, T. Sunagawa, H. Nakajima, H. Watanabe, S. Fujitani, K. Nishio, Extended Abstract of the 39th Battery Symposium in Japan, Sendai, Japan, 25–27 November 1999, p. 315.
[12] W. Li, C. Currie, J. Electrochem. Soc. 144 (1997) 2773.
[13] S.P. Sheu, C.Y. Yao, J.M. Chen, Y.C. Chiou, J. Power Sources 68 (1997) 533.
[14] H. Wang, Y.-I. Jang, B. Huang, D.R. Sadoway, Y.-M. Chiang, J. Electrochem. Soc. 146 (1999) 473.
[15] J. Cho, B. Park, J. Power Sources 92 (2001) 35.
[16] K. Dokko, M. Nishizawa, S. Horikoshi, T. Itoh, M. Mohamed, I. Uchida, Electrochem. Solid State Lett. 3 (1999) 3.
[17] J. Cho, H. Jung, Y. Park, G. Kim, H.S. Lim, J. Electrochem. Soc. 147 (2000) 15.